

Seasonality in dominant upper-ocean dynamics at submesoscales

Cesar, Sarah, Teri, & Bill¹

Key Points.

- Submesoscale (10-100 km) vertical vorticity and lateral strain peaks in late Winter/early Spring; divergence and stratification peaks in late Summer/early Fall.
- Quasi-balanced eddies dominate the variability in late Winter/early Spring; inertia-gravity waves dominate in late Summer/early Fall.
- These results have implications for the diagnosis of surface velocity from high-resolution altimeters.

(Type abstract here)

1. Introduction

1.1. Motivation

Recent studies have suggested that submesoscale upper-ocean flows undergo strong seasonal cycle [Sasaki *et al.*, 2014; Qiu *et al.*, 2014; Callies *et al.*, 2015; Thompson *et al.*, 2016; Buckingham *et al.*, 2016].

Observations at submesoscales are limited.

SWOT and COMPIRA will provide submesoscale-resolving SSH measurements with global coverage.

1.2. This paper

Using the output of a $1/24^\circ$ state estimate, we show that (vertical) vorticity and (horizontal) divergence undergo strong seasonal cycle that are out of phase. This seasonal cycle is associated with changes in the upper-ocean stratification. As previously argued, in late Winter/early Spring, deep mixed-layers are prone to shallow baroclinic instabilities that are roughly in geostrophic balance and flux energy upscale [Sasaki *et al.*, 2014; Callies *et al.*, 2016], driving a mild seasonal modulation at mesoscales [Sasaki *et al.*, 2014; Qiu *et al.*, 2014]. The divergence part of the flow, however, peaks in late Summer/early Fall, when the upper-ocean is strongly stratified. Hence these results suggest a strong seasonal modulation of the dominant upper-ocean submesoscale dynamics with the dominance quasi-balanced turbulence in late Winter/early Spring and quasi-linear inertia-gravity waves in late Summer/early Fall.

2. The LLC2160 model output

We use the output of the latitude-longitude polar cap (LLC) MITgcm numerical simulation. The output analyzed here, the LLC2160, is the $1/24^\circ$ — 90-vertical-levels simulation from a hierarchy of global forward numerical solutions on a LLC grid [Forget *et al.*, 2015] that were spun up from a ECCO2 adjoint-method state estimate. The LLC2160 was forced by tides and high-resolution surface fluxes similarly to the LLC4320 simulation used by Rocha *et al.* [2016] — see their appendix D. We chose the second-higher resolution simulation (LLC2160) of the LLC hierarchy because it was run for longer: the LLC2160 output spans

two years from March 2011 to April 2013. The model time-step was 45s and the model variables were saved hourly. LLC hierarchy setup and control files are available online (at http://mitgcm.org/viewvc/MITgcm/MITgcm_contrib/llc_hires). For the LLC hierarchy, the sea-surface height is calculated using a linearized equation. The model output was provided by D. Menemenlis (JPL/NASA).

A key aspect of the simulation analyzed here is that it is forced by the 16 most significant tidal components. Barotropic tides interact with topography and generate internal tides that project on mesoscales to submesoscales [Rocha *et al.*, 2016]. Hence, tidal forcing fundamentally differentiates our analysis from recent modeling studies that investigated upper dynamics and its seasonality [Sasaki *et al.*, 2014; Qiu *et al.*, 2014].

The region of focus is the northwest Pacific, in the vicinities of the Kuroshio Extension, where previous studies have shown strong seasonality in the quasi-geostrophic surface velocity field. We analyze a sub-domain of the LLC2160 simulation of about 2000 km^2 spanning $155\text{--}175^\circ\text{E}$; $25\text{--}40^\circ\text{N}$ (figure 1a-b).

3. Seasonality in surface velocity and near-surface stratification

Focusing on the lateral gradients of the horizontal velocity vector. The lateral gradients are calculated using a centered second-order finite differences scheme. We then calculate the vertical vorticity $\zeta \equiv v_x - u_y$, horizontal divergence $\delta \equiv u_x + v_y$, and the magnitude of the lateral rate of strain $S \equiv [(v_x + u_y)^2 + (u_x - v_y)^2]^{1/2}$. These quantities highlight the submesoscale structures in the flow and hint on their dynamics.

Figures 1a-b show snapshots of vertical vorticity ζ in early Spring (April 15) and Fall (October 15). Clearly, a strong seasonality in vorticity exists: large values of fine-grained vertical vorticity are observed in early Spring with maximum values as high as $0.9f$, where f is the local planetary vorticity, and root-mean-square (RMS) of about 0.25. In early Fall, the situation is the opposite: the vertical vorticity is coarse-grained, and its local maximum and RMS is no larger than $0.3f$ and $0.1f$, respectively. Indeed, the seasonal cycle in vorticity/strain is very strong (Figure 2): the RMS vertical vorticity is about twice as large in late Winter/early Spring than it is in late Summer/early Fall. This picture is consistent with recent studies: shallow baroclinic instabilities energize the submesoscales in late Winter, drawing from the available potential energy stored in deep mixed layers [Sasaki *et al.*, 2014; Callies *et al.*, 2015, 2016].

¹Scripps Institution of Oceanography, University of California San Diego, La Jolla, CA, USA

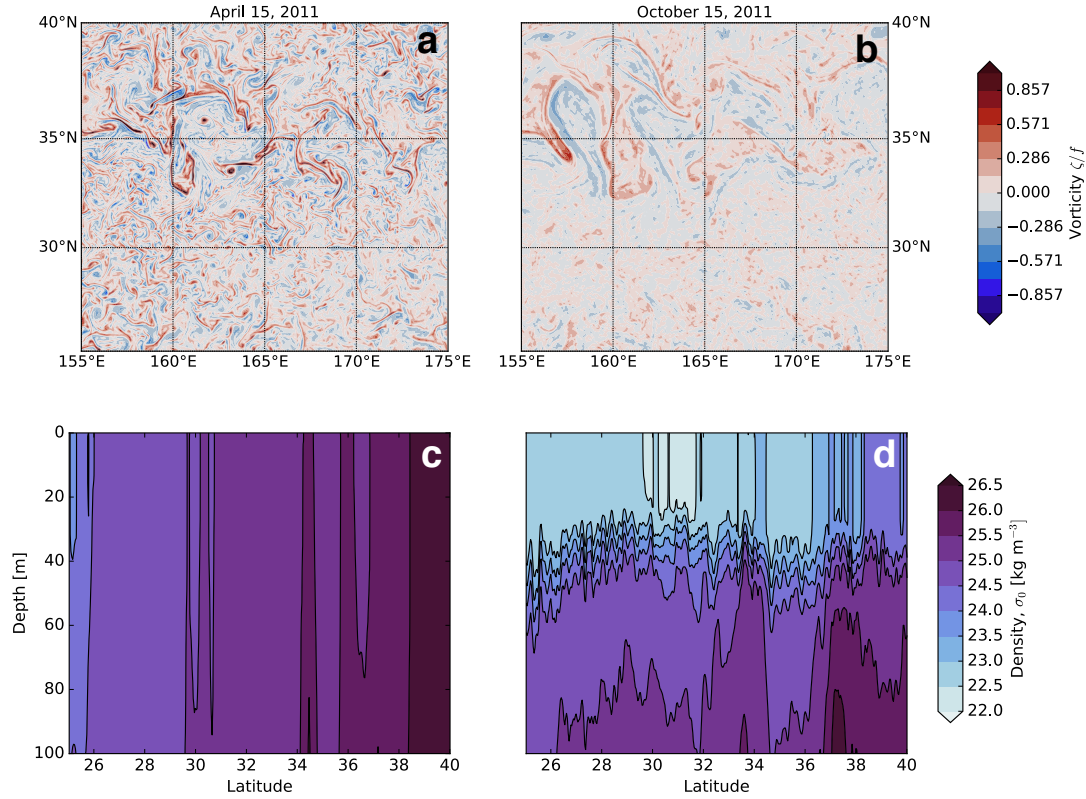


Figure 1. Snapshots of surface vorticity (a and b) and a transect of potential density at 165°E (c and d). The snapshots were taken at 00:00 UTC.

The bulk of the vertical vorticity is associated with subinertial flows ($T_f = 2\pi/f_0 \approx 23.5h$, where f_0 is the inertial frequency at the mean latitude): daily-averaging the velocity fields reduces the vertical vorticity by less than 20% and the seasonal cycle remains strong (see green lines in figure 2). Most of this seasonal cycle is associated with submesoscale flows: low-pass filtering the velocity field with a cut-off scale of 100 km reduces the RMS vorticity by at least 40%, yielding bulk statistics of velocity gradient roughly consistent with AVISO geostrophic velocity data (see lines blue and black in figure 2).

The horizontal divergent part of the flow is significant: the RMS is $\delta/f > 0.1$). Most of these horizontal divergent flows project are supra-inertial and project on scales smaller than 100 km: daily-averaging the velocity fields or low-pass filtering (100 km cutoff) reduces the horizontal divergence by about 70%. Furthermore, the seasonal cycle in horizontal divergence is out-of-phase with that of vertical vorticity: the horizontal divergence is about 30% larger in late Summer/early Fall than it is in late Winter/early Spring. The divergence associated with submesoscale subinertial eddies is small and its seasonal cycle is in phase with that of vorticity (see green lines). The seasonal cycle of the horizontal divergence is roughly in phase with the seasonal cycle of the near-surface (0-50m) stratification.

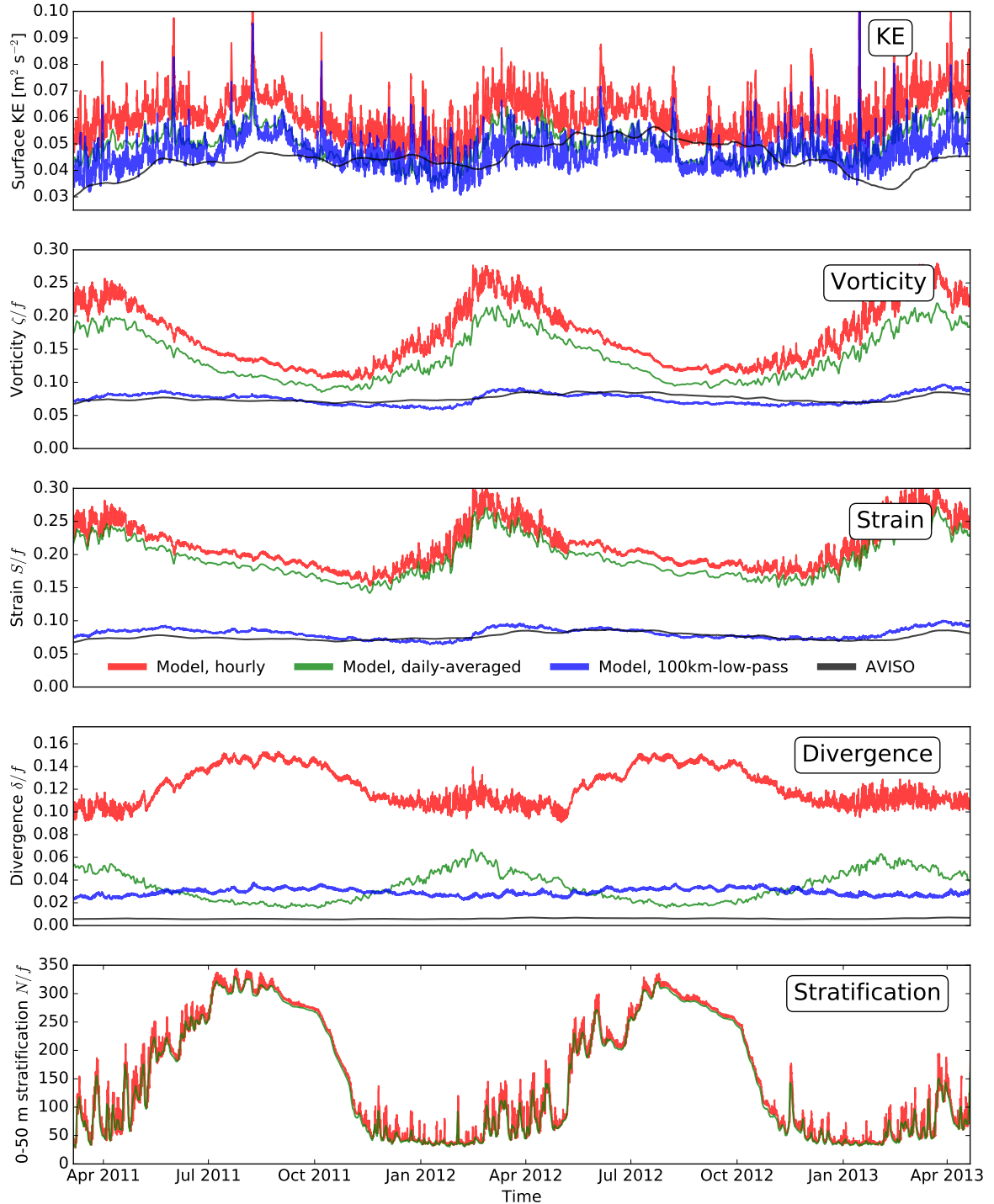


Figure 2. Time series of the root-mean-square of kinetic energy (a), vorticity (b), lateral strain (c), horizontal divergence (d), and stratification in the upper 50 m (e).

4. Projection on horizontal scales

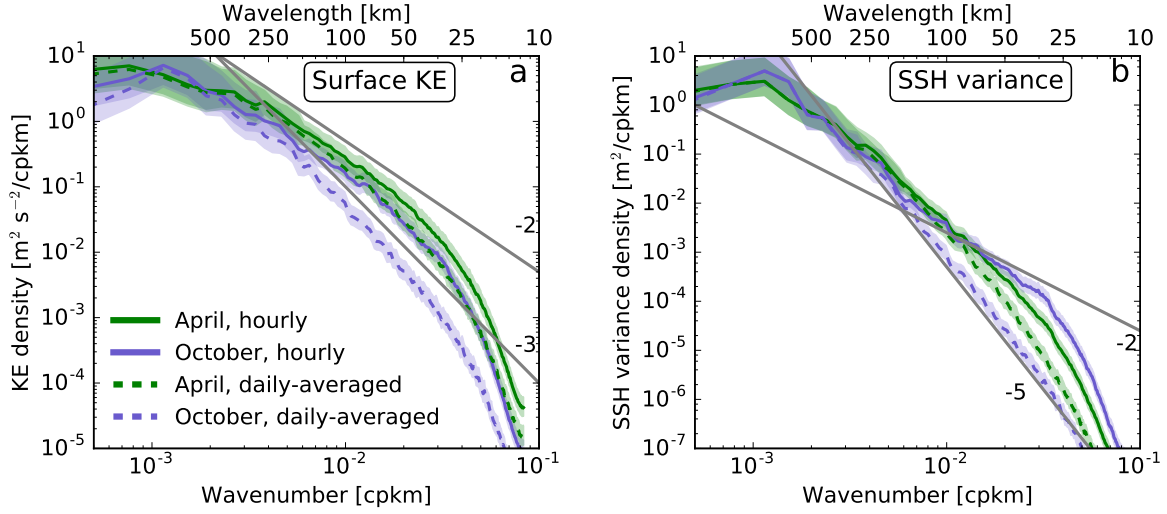


Figure 3. Surface (horizontal) KE and SSH variance wavenumber spectra. Solid lines are spectra based on hourly snapshots, dashed lines are spectra based on daily-averaged fields.

ber spectra of kinetic energy and sea-surface height (SSH) variance.

5. Projection on time scales

To better understand the dynamics the projection of these flows on horizontal scales, we calculate wavenum-

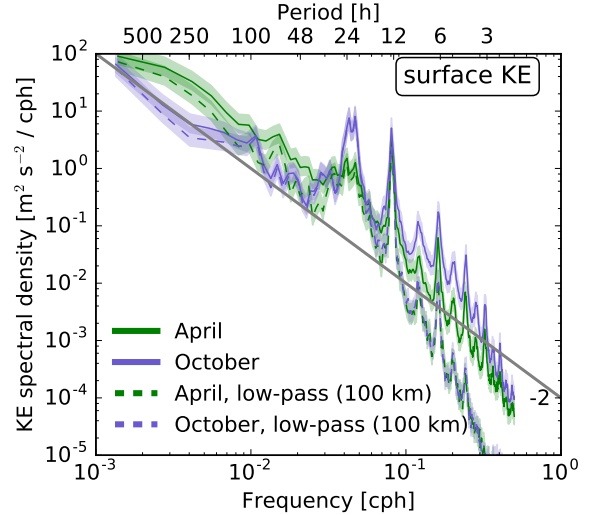


Figure 4. Surface (horizontal) KE frequency spectra. Solid lines are spectra based on the $1/24^\circ$ fields, dashed line are spectra based on 100-km-low-pass smoothed fields.

6. Summary and Discussion

Our main finding is that upper-ocean divergent flows, dominated by inertia-gravity waves, undergo a strong seasonal cycle that is out-of-phase with the seasonal cycle of the quasi-balanced flows. Therefore, the present results suggest significant seasonal modulation of the dominant upper-ocean dynamics at submesoscales (10–100 km): Quasi-balanced turbulence driven by shallow baroclinic instabilities in late Winter/early Spring and inertia-gravity waves dominate in late Summer/early Fall.

That the surface velocity and SSH submesoscale (10–100 km) variability may be dominated by ageostrophic flows in Summer/Fall has consequences for the interpretation of data from the future SWOT and COMPIRA altimeter missions, which will deliver SSH measurements at submesoscales. To the extent that high-frequency flows are dominated by incoherent internal tides and other internal waves, it may be very difficult (if not impossible) to separate submesoscale SSH variability associated with geostrophic motions from high-frequency, ageostrophic flows. Thus, previous claims that one will be able to easily obtain submesoscale surface geostrophic velocities and monitor such seasonal cycle on global scales [Sasaki *et al.*, 2014; Qiu *et al.*, 2014] are overstated.

The present analysis focuses on a single patch of ocean in the vicinities of the Kuroshio Extension, not representative of other regions such as eastern boundary currents and the middle of the subtropical gyre: care must be taken in overgeneralizing these results with care. The effects of smaller-scale/higher-frequency

“sub-submesoscale” flows on the submesoscale surface velocity and SSH variability are presently unknown.

Acknowledgments. Thanks to D. Menemenlis (JPL/NASA) and the other MITgcm usual suspects. This research was funded by NSF and NASA.

References

- Buckingham, C. E., A. C. Naveira Garabato, A. F. Thompson, L. Brannigan, A. Lazar, D. P. Marshall, A. George Nurser, G. Damerell, K. J. Heywood, and S. E. Belcher (2016), Seasonality of submesoscale flows in the ocean surface boundary layer, *Geophysical Research Letters*, 43(5), 2118–2126.
- Callies, J., R. Ferrari, J. M. Klymak, and J. Gula (2015), Seasonality in submesoscale turbulence, *Nature communications*, 6.
- Callies, J., G. Flierl, R. Ferrari, and B. Fox-Kemper (2016), The role of mixed-layer instabilities in submesoscale turbulence, *Journal of Fluid Mechanics*, 788, 5–41.
- Forget, G., J.-M. Campin, P. Heimbach, C. Hill, R. Ponte, and C. Wunsch (2015), Ecco version 4: an integrated framework for non-linear inverse modeling and global ocean state estimation, *Geosci. Model Dev.*, 8, 3071–3104.
- Qiu, B., S. Chen, P. Klein, H. Sasaki, and Y. Sasai (2014), Seasonal mesoscale and submesoscale eddy variability along the north pacific subtropical countercurrent, *Journal of Physical Oceanography*, 44(12), 3079–3098.
- Rocha, C. B., T. K. Chereskin, S. T. Gille, and D. Menemenlis (2016), Mesoscale to submesoscale wavenumber spectra in drake passage, *Journal of Physical Oceanography*, 46, 601–620.
- Sasaki, H., P. Klein, B. Qiu, and Y. Sasai (2014), Impact of oceanic-scale interactions on the seasonal modulation of ocean dynamics by the atmosphere, *Nature communications*, 5.
- Thompson, A. F., A. Lazar, C. Buckingham, A. C. Naveira Garabato, G. M. Damerell, and K. J. Heywood (2016), Open-ocean submesoscale motions: A full seasonal cycle of mixed layer instabilities from gliders, *Journal of Physical Oceanography*, 46(4), 1285–1307.